nature microbiology

Article

https://doi.org/10.1038/s41564-026-02288-5

Conditional activation of Cas13 enforces lysogeny in a native type VI-A CRISPR host

Received: 11 April 2025

Accepted: 10 February 2026

Published online: 10 March 2026

Check for updates

Marshall Godsil, Nova Wei & Alexander J. Meeske

CRISPR–Cas (clustered regularly interspaced short palindromic repeats and CRISPR-associated proteins) systems present a barrier to prophage acquisition by restricting invading phages or by inducing autoimmune cleavage of integrated prophage DNA. The RNA-sensing type VI CRISPR nuclease Cas13 mediates non-specific RNA cleavage upon recognition of phage lytic transcripts, but how this system influences the temperate phage life cycle remains unknown. Here we report that the *Listeria seeligeri* type VI-A CRISPR system restricts the lytic cycle of temperate phages but tolerates prophage acquisition and interferes with prophage induction through a non-abortive mechanism. During attempts at induction, Cas13 activation forces prophage re-integration, thus maintaining lysogeny. We also find that during polylysogenic induction, Cas13 acts specifically, restricting only the targeted phage, in contrast to its behaviour during lytic replication. Our findings show that Cas13 elicits a unique response to each stage of the temperate phage life cycle, enabling type VI CRISPR hosts to acquire potentially beneficial prophages while mitigating lysis.

Bacteria have evolved a diverse catalogue of immune systems to defend against genetic parasites[1]. Such foreign genetic elements include temperate phages, which colonize 50–75% of bacteria[2,3]. Temperate phages replicate through either the lytic cycle, producing virions and lysing their hosts, or the lysogenic cycle, integrating into the host chromosome as a prophage[4]. During lysogeny, prophages silence the bulk of lytic genes. The lytic and lysogenic pathways are connected through prophage induction, where an integrated prophage excises from the host chromosome and initiates lytic replication, usually in response to stressors like DNA damage. Prophages express non-essential accessory genes during lysogeny, which can enhance host fitness by restricting super-infecting phages, facilitating colonization of new environments and enhancing bacterial pathogenicity[5–7]. While virtually all bacterial immune systems restrict the phage lytic cycle, whether and how they influence lysogeny and prophage induction remains relatively uncharacterized.

CRISPR–Cas (clustered regularly interspaced short palindromic repeats and CRISPR-associated proteins) systems provide anti-phage immunity to bacterial hosts using diverse RNA-guided Cas nucleases (types I–VII) which sense and degrade target viral nucleic acids[8–10]. Short sequences derived from phage genomes, called spacers, are transcribed from the CRISPR array and processed into small crRNAs (CRISPR RNAs) that recognize homologous sequences in phage genomes or transcripts. Active DNA-sensing CRISPR systems are incompatible with targeted prophages, as cleavage of the integrated phage genome is lethal to the host[11–13]. Previous work showed that type I-F CRISPR targeting of temperate phages in *Pseudomonas aeruginosa* leads to prophage cleavage following integration, inducing growth defects, and loss of the CRISPR system[13]. By contrast, the RNA-sensing type III-A CRISPR system of *Staphylococcus epidermidis* allows prophage acquisition when targeted phage genes remain silenced[14]. Once activated, however, type III-A systems cleave both RNA and DNA[15–17]. Any target transcription during lysogeny thus induces type III-A -mediated cleavage of the integrated prophage DNA, resulting in growth defects[18]. Thus, research to date has shown that CRISPR systems pose a barrier to prophage acquisition and that autoimmune cleavage of integrated prophage DNA drives CRISPR-mediated fitness costs.

In contrast to other CRISPR–Cas types, the Cas13 nuclease of type VI-A systems exclusively recognizes and cleaves RNA. This raises the possibility that type VI-A immunity might allow prophage acquisition, similar to the type III-A system, while avoiding autoimmune DNA cleavage[19,20]. In the native type VI-A host *Listeria seeligeri*,

Department of Microbiology, University of Washington, Seattle, WA, USA. e-mail: meeske@uw.edu

https://doi.org/10.1038/s41564-026-02288-5

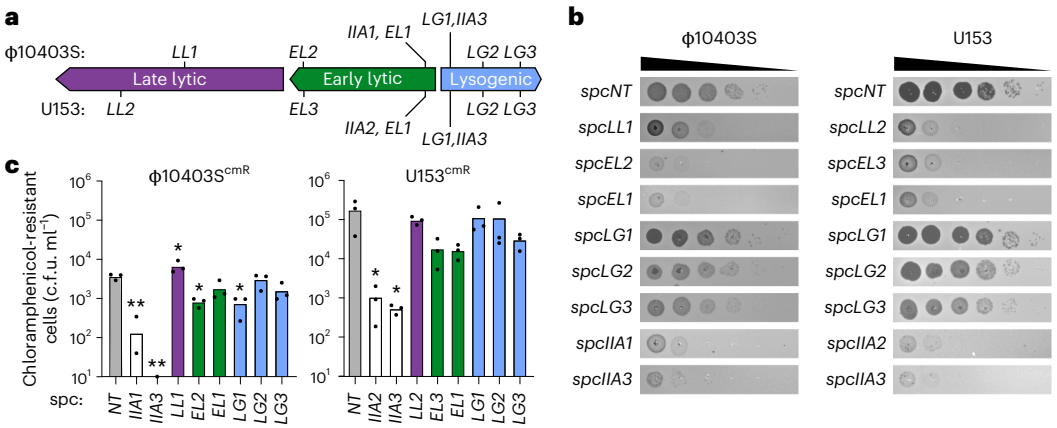

Fig. 1 | The type VI-A CRISPR system tolerates lysogeny. a, Diagram of type VI-A and type II-A spacer target locations in the ϕ10403S and U153 phage genomes. **b**, Plaque assays of ϕ10403S and U153 on lawns of *L. seeligeri* harbouring a non-targeting spacer (*spcNT*) or individual type VI-A or type II-A spacer. Three biological replicates were performed, and representative images are shown. **c**, Chloramphenicol-resistant c.f.u. representing lysogenization events were enumerated following infection of noted strains with cmR-marked ϕ10403S or U153. Three biological replicates and their means are shown. One-way analyses of variance (ANOVA) with Dunnet's tests were performed to compare the means of each spacer containing strain to the *spcNT* control (grey); $^{*}P < 0.05$ denotes a significant difference between the indicated column and the *spcNT* control column; $^{**}P < 0.01$; no asterisk represents a non-significant difference. Exact *P* values for **c** are as follows: for ϕ10403S^{cmR} infections: *spcIIA1*, 0.0039; *spcIIA3*, 0.0029; *spcLL1*, 0.0134; *spcEL2*, 0.0215; *spcLG1*, 0.0179; for U153^{cmR} infections: *spcIIA2*, 0.0414; *spcIIA3*, 0.0407.

Cas13-mediated recognition of phage lytic transcripts leads to non-specific degradation of phage and host messenger RNA, halting both the phage lytic cycle and growth of the infected host[21]. Thus, Cas13 acts via abortive infection: growth-arrested cells limit viral replication, halting phage spread to uninfected cells in the population. We also previously reported that cells can be resuscitated from Cas13-mediated growth arrest if co-resident restriction endonucleases degrade the targeted phage genome, removing the source of target transcripts[22]. Here we report that the type VI-A CRISPR system of *L. seeligeri* tolerates lysogenization by targeted prophages. Furthermore, upon induction of targeted prophages, we find that Cas13 prevents completion of the phage lytic cycle, instead enforcing re-integration and retention of the prophage. This process does not affect viability of the host cell, revealing a non-abortive effect of the type VI-A CRISPR system. Finally, during induction of polylysogenic hosts containing multiple distinct prophages, Cas13 specifically restricts induction of the targeted prophage, in contrast to its non-specific activity during lytic infection. Taken together, our data indicate that type VI-A CRISPR systems enable prophage acquisition and retention while simultaneously restricting lytic infection and prophage induction.

Results

Type VI-A CRISPR tolerates integration of temperate phages

We began by investigating the consequences of type VI-A CRISPR targeting on the life cycle of temperate phages in a prophage-free *L. seeligeri* strain, LS1. We individually introduced a collection of spacers into the LS1 chromosome, directing natively encoded Cas13 to sense lysogenic (*LG*), early lytic (*EL*) or late lytic (*LL*) transcripts of two related temperate *Listeria* phages: ϕ10403S and U153 (Fig. 1a and Extended Data Fig. 1)[23]. The predicted function of targeted transcripts is documented in Supplementary Table 1. We also tested interference by a DNA-sensing *Listeria* type II-A CRISPR–Cas system ectopically integrated into the LS1 genome, programmed to target either a lytic or lysogenic gene. Upon infection of these strains, we observed that all type II-A spacers and specifically those type VI-A spacers matching lytic transcripts strongly reduced plaque formation by both phages (Fig. 1b and Supplementary Fig. 1). Type VI-A spacers sensing lysogenic transcripts did not impact plaque formation (Fig. 1b), despite being functional in interference against target-expressing plasmids (Extended Data Fig. 2). These data show that type VI-A detection of RNA targets leads to stark differences in temperate phage restriction dependent on protospacer context, similar to the type III-A CRISPR system[14].

Next, to evaluate the effect of type VI-A immunity on lysogenization by temperate phage, we engineered a constitutively expressed chloramphenicol resistance (cmR) gene into non-essential regions of the ϕ10403S and U153 genomes. We used these phages to infect strains containing the type VI-A or II-A spacers listed above and immediately selected for chloramphenicol-resistant colonies to enumerate lysogen formation. For both phages, we observed that type II-A CRISPR immunity reduced lysogen formation by 25- to 1,000-fold compared to a non-targeting spacer. By contrast, type VI-A CRISPR was more tolerant of prophage acquisition, ranging from a depletion of 11-fold to a 1.8-fold increase (Fig. 1c). Type VI-A spacers targeting late lytic genes had little to no effect on lysogeny, which is logical, as transcription of late lytic targets is not expected to occur before prophage integration. Spacers targeting early lytic genes showed up to an 11-fold reduction in lysogen formation, suggesting these genes may be transcribed before lysogenic commitment. Finally, spacers targeting lysogenic genes, including putative integrase and repressor, had surprisingly modest effects on lysogeny. Using RNA sequencing (RNA-seq), we confirmed that lysogenic targets are detectably expressed during bulk infection (Extended Data Fig. 3), suggesting that lysogenic transcripts are produced but in insufficient quantities to activate Cas13. Taken together, our data indicate that Cas13 restricts lytic infection, dependent on protospacer context, but tolerates prophage acquisition. This is in contrast to the RNA-sensing, DNA-cleaving type III-A system, which restricts prophage acquisition when sensing lysogenic transcripts and shows incomplete tolerance when sensing lytic transcripts[14,18].

Conditional activation governs Cas13 tolerance to lysogeny

Previous work on *Leptotrichia shahii* Cas13 expressed in *Escherichia coli* showed that a threshold level of target expression is required for nuclease activation[24]. Our observations of prophage tolerance by Cas13 suggested a similar principle governs Cas13 activation in *L. seeligeri*. To investigate this, we used a strain of *L. seeligeri* harbouring a Cas13-targeted transcript under the P_{tet} inducible promoter (LS1 94°::P_{tet}-*pspc4*)[21]. We incubated this strain with various concentrations of anhydrotetracycline (aTc) inducer and measured resultant growth defects by OD_{600} (optical density at 600 nm) at 16 h after incubation

https://doi.org/10.1038/s41564-026-02288-5

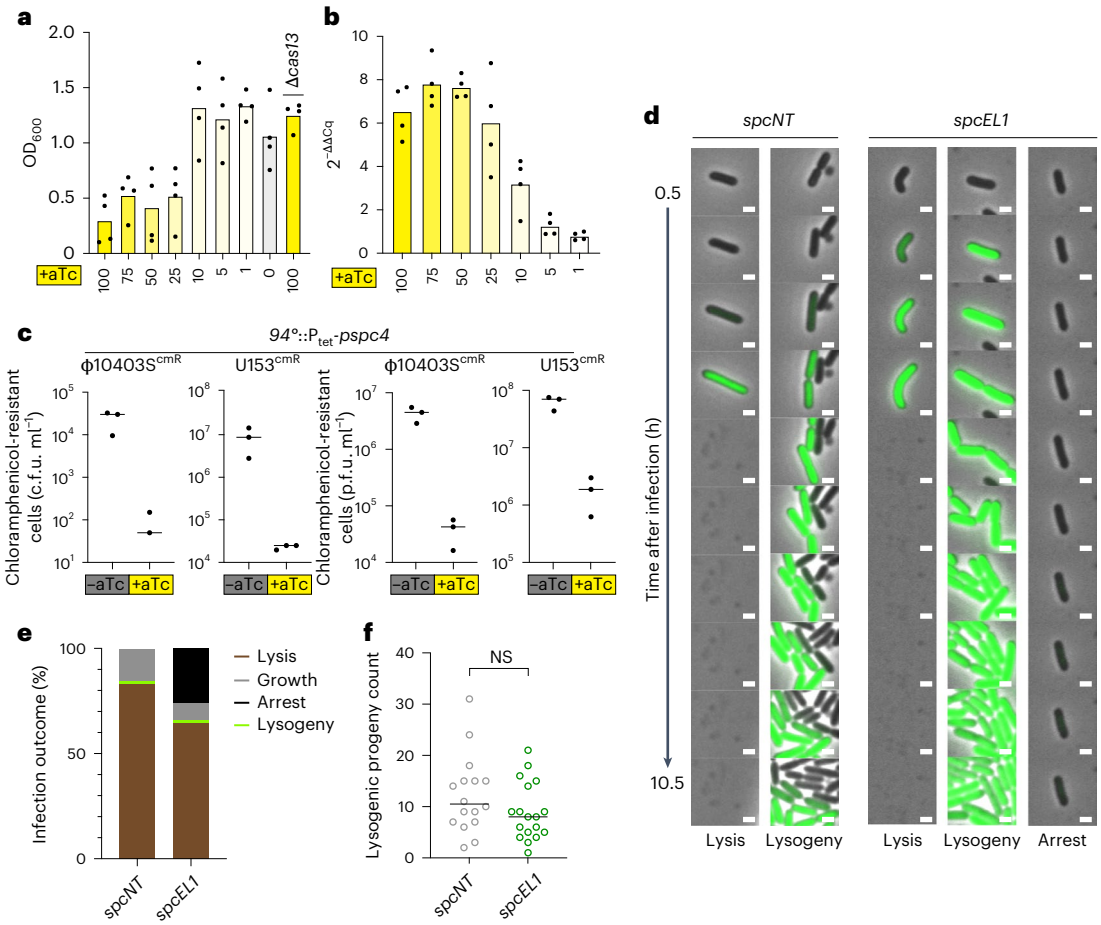

Fig. 2 | Targeted phages integrate without activating Cas13. a, For replicate cultures of LS1 94°::Ptet-*pspc4*, OD_{600} was measured after 16 h of incubation with the indicated concentration of inducer (aTc, ng ml^{-1}); the rightmost column denotes an isogenic control with Cas13 deleted at 100 ng ml^{-1} aTc. **b**, Following incubation of LS1 94°::Ptet-*pspc4*Δ*cas13* strain with various concentrations of inducer (aTc), target transcript abundance was quantified using RT-qPCR. Here, $2^{-\Delta\Delta Cq}$ is relative expression of the *pspc4* target normalized to expression of the housekeeping gene *ssbA*, then normalized to a control lacking aTc. Four biological replicates and their means are shown for **a** and **b**. **c**, Restriction of lysogen formation after Cas13 pre-activation. *L. seeligeri* LS1 94°::Ptet-*pspc4* strains were infected with ϕ10403S-cmR or U153-cmR in the presence or absence of inducer (aTc); resulting cmR c.f.u. and p.f.u. were enumerated. Three biological replicates and their means are shown. **d**, Montages of *L. seeligeri* cell fates following infection with ϕ10403S-mStayGold in a *spcNT* or *spcEL1* background. Scale bars, 1 μm. **e**, Cell fates were manually tracked and assigned for 600 cells from 2 biological replicates for each background. **f**, For cells that became lysogenic, progeny cells were counted at 8 h to quantify initial growth rate during lysogen formation in *spcNT* or *spcEL1* background. Each circle represents the number of lysogenic progeny produced from a single infected progenitor cell, representing a biological replicate (*spcNT* $n = 16$, *spcEL1* $n = 18$). A two-sided Student's *t*-test was performed to compare the means of the two conditions; NS denotes a non-significant difference.

(Fig. 2a). We detected equally strong Cas13-induced growth defects for cultures incubated with >25 ng ml^{-1} aTc, while no effect was observed with lower aTc concentrations (Fig. 2a). In parallel, we incubated an isogenic strain lacking Cas13 (LS1 94°::P$_{tet}$-*pspc4 Δcas13*) with identical aTc concentrations and measured abundance of target transcripts at 5 min after induction by real-time quantitative PCR (RT-qPCR) (Fig. 2b). In contrast to the precipitous appearance of a Cas13-induced growth defect, target RNA expression increased gradually with aTc concentration, hitting saturation at 75 ng ml^{-1} aTc (Fig. 1b). These data argue that activation of Cas13 in *L. seeligeri* is gated and that low levels of target expression are tolerated.

Next, we tested whether prophage tolerance is due to a lack of sufficient target expression necessary to activate Cas13, or the inability of active Cas13 to interfere with lysogen establishment. Using the 94°::P$_{tet}$-*pspc4* strain described above, we induced Cas13 activation with 100 ng ml^{-1} aTc 30 min before infecting with cmR-marked phages, measuring lysogen and p.f.u. (plaque-forming units) formation (Fig. 2c). For both phages, we observed equal ~100-fold reductions in p.f.u. and lysogen titres when Cas13 was pre-activated. Our data indicate that when activated, Cas13 is competent to restrict prophage acquisition. Thus, prophage tolerance during natural type VI targeting results from a lack of Cas13 activation.

To further investigate the status of Cas13 activation during lysogen formation, we tracked the growth of phage-infected cells by time-lapse microscopy. As Cas13 activation induces a dramatic growth arrest, we expected that even temporary Cas13 activation during lysogen establishment would manifest as delayed growth in incipient lysogens. We inserted a constitutively expressed fluorescent protein, mStayGold, into a non-essential region of ϕ10403S for visualization of infection. We loaded cells infected with ϕ10403S-mStayGold at a multiplicity of infection (MOI) of 50 into a microfluidic chamber and imaged them over the course of 12 h. In the presence of a non-targeting spacer (*spcNT*), we visualized lysis of infected cells, outgrowth of uninfected cells and growth of lysogenic cells into microcolonies showing green fluorescence (Fig. 2d). We also observed these fates with three lytic targeting spacers with the additional outcome of Cas13-induced growth arrest. While lysogeny was rare, we found that rates did not substantially differ between our *spcNT*, *spcEL1* and *spcLL1* strains (Fig. 2e and Supplementary Fig. 2), as observed in bulk lysogenization assays (Fig. 1c). To determine whether Cas13 is activated transiently during

https://doi.org/10.1038/s41564-026-02288-5

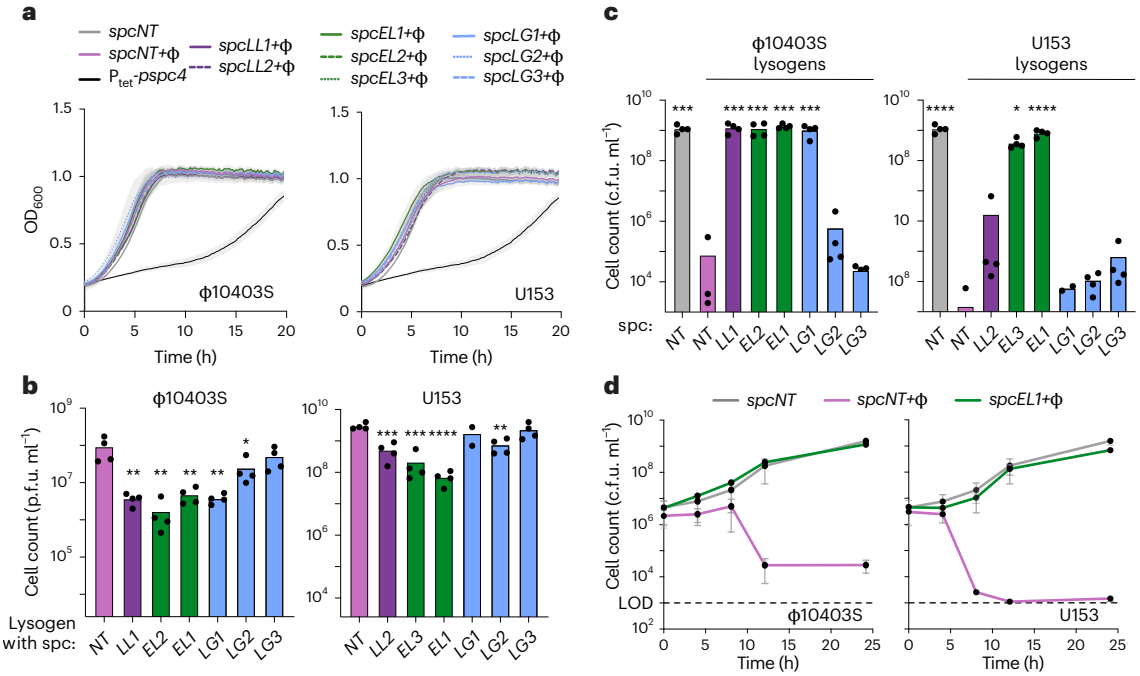

Fig. 3 | Type VI CRISPR immunity limits prophage induction and enhances cell survival. a, OD_{600} growth curves of self-targeting lysogens. Left: ϕ10403S lysogens. Right: U153 lysogens. The indicated strains were cultured to mid-log phase and diluted in BHI, and OD_{600} was measured for 20 h. Lines represent the mean of four biological replicates, with grey shaded areas representing the s.e.m. (standard error of the mean). **b**, Production of p.f.u. by ϕ10403S or U153 lysogens harbouring the indicated spacer, or a *spcNT* non-lysogen control (grey); p.f.u. were enumerated at 8 h after treatment with MMC (pulsed at 2 mg ml^{-1} for 60 min). **c**, Corresponding production of c.f.u. was enumerated for the indicated strains at 24 h after MMC treatment. For **b** and **c**, individual biological replicates are shown. For **b** and **c**, one-way ANOVA analyses with Dunnet's tests were performed to compare the means of each spacer containing strain to the *spcNT* lysogen (pink); $^{*}P < 0.05$ denotes a significant difference between the indicated column and the *spcNT* lysogen; $^{**}P < 0.01$; $^{***}P < 0.001$; $^{****}P < 0.0001$; no asterisk represents a non-significant difference. **d**, Time course of viable c.f.u. count after MMC treatment (pulsed at 2 mg ml^{-1} for 60 min) of the indicated strains. LOD, limit of detection. Mean and s.e.m. of three biological replicates are shown. Exact *P* values for **b** are as follows: for ϕ10403S reactivations: *spcLL1*, 0.0015; *spcEL2*, 0.0012; *spcEL1*, 0.0017; *spcLG1*, 0.0015; *spcLG2*, 0.0155; for U153 reactivations: *spcLL2*, 0.0006; *spcEL3*, 0.0002; *spcEL1*, <0.0001; *spcLG2*, 0.00717. Exact *P* values for **c** are as follows: for ϕ10403S reactivations: *spcLL1*, 0.0001; *spcEL2*, 0.0003; *spcEL1*, 0.0001; *spcLG1*, 0.001; for U153 reactivations: *spcEL3*, 0.0135; *spcEL1*, <0.0001.

lysogen formation, resulting in a growth delay, we tracked the growth rate of lysogens formed by counting their progeny at 8 h after infection. We found that there was no detectable difference in lysogenic progeny count at 8 h between *spcNT* and *spcEL1* cells (Fig. 2f), confirming that lysogens form without activating Cas13.

Cas13 immunity enables cell survival from prophage induction

While our data indicate that prophage acquisition is tolerated in the presence of type VI-A immunity, we wondered whether these strains would show growth defects like those observed with other CRISPR types. We performed growth curves with lysogens harbouring a non-targeting spacer, or a spacer targeting the integrated prophage, hereafter referred to as 'self-targeting lysogens'. As a comparison, we measured growth of the 94˚::P$_{tet}$-*pspc4* strain incubated with 100 ng ml^{-1} aTc. We found that self-targeting lysogens showed no detectable growth defect during exponential growth, while Cas13 activation in the 94˚::P$_{tet}$-*pspc4* strain led to severe growth defects (Fig. 3a). We also tracked prophage retention over 4 days by passaging self-targeting or non-targeting lysogens harbouring the ϕ10403S-mStayGold prophage; we saw that the prophage was stably maintained at equal proportions in both backgrounds (Extended Data Fig. 4). Our data indicate that self-targeting by the type VI-A CRISPR system is not associated with an intrinsic fitness cost.

Next, we investigated the fates of phages and cells undergoing prophage induction in the presence of type VI-A CRISPR interference. We enumerated p.f.u. released from self-targeting or non-targeting lysogens following a 60 min treatment with the DNA-damaging agent mitomycin C (MMC). Eight hours after MMC treatment, we observed Cas13-dependent reductions in phage released from lysogens containing lytic transcript targeting spacers (Fig. 3b). These strains also produced fewer p.f.u. from spontaneous induction, in the absence of MMC (Extended Data Fig. 5). In our induction experiments, we noted particularly robust survival of lysogens harbouring lytic gene-targeting spacers 24 h after MMC treatment. (Fig. 3c). To further investigate this, we tracked colony-forming units (c.f.u.) over time following treatment with MMC in ϕ10403S and U153 self-targeting lysogens, along with a non-lysogen control (Fig. 3d and Extended Data Fig. 6). Both non-targeting lysogens showed severe drops in viability following MMC treatment. Strikingly, the survival of both *spcEL1* lysogens was indistinguishable from non-lysogens at all time points (Fig. 3d), indicating a lack of widespread lysis or growth arrest. This phenotype was consistent in multiple spacer contexts (Extended Data Fig. 6). This suggests that during prophage induction, Cas13 restricts phage replication in a non-abortive fashion, contrary to its effect during lytic replication. We also determined that both ϕ10403S and U153 confer immunity to cognate super-infecting phages using locked-in, integrase deficient Δ*int* prophages (Extended Data Fig. 7a). This shows that Cas13-dependent survival is not caused by protection from secondary infection, as lysogens are already immune to this. Furthermore, we found that cell death during induction is unaffected by host mutations in the phage receptor (*ggaB*), indicating that lysis does not result from secondary infection or lysis-from-without (Extended Data Fig. 7b). We also found that Cas13 enhances host survival during induction of two other distinct prophages, ϕEGDe and ϕLS46 (Extended Data Figs. 1 and 8). Taken together, our data indicate that prophage targeting by Cas13 enables survival from induction, without substantial growth arrest.

https://doi.org/10.1038/s41564-026-02288-5

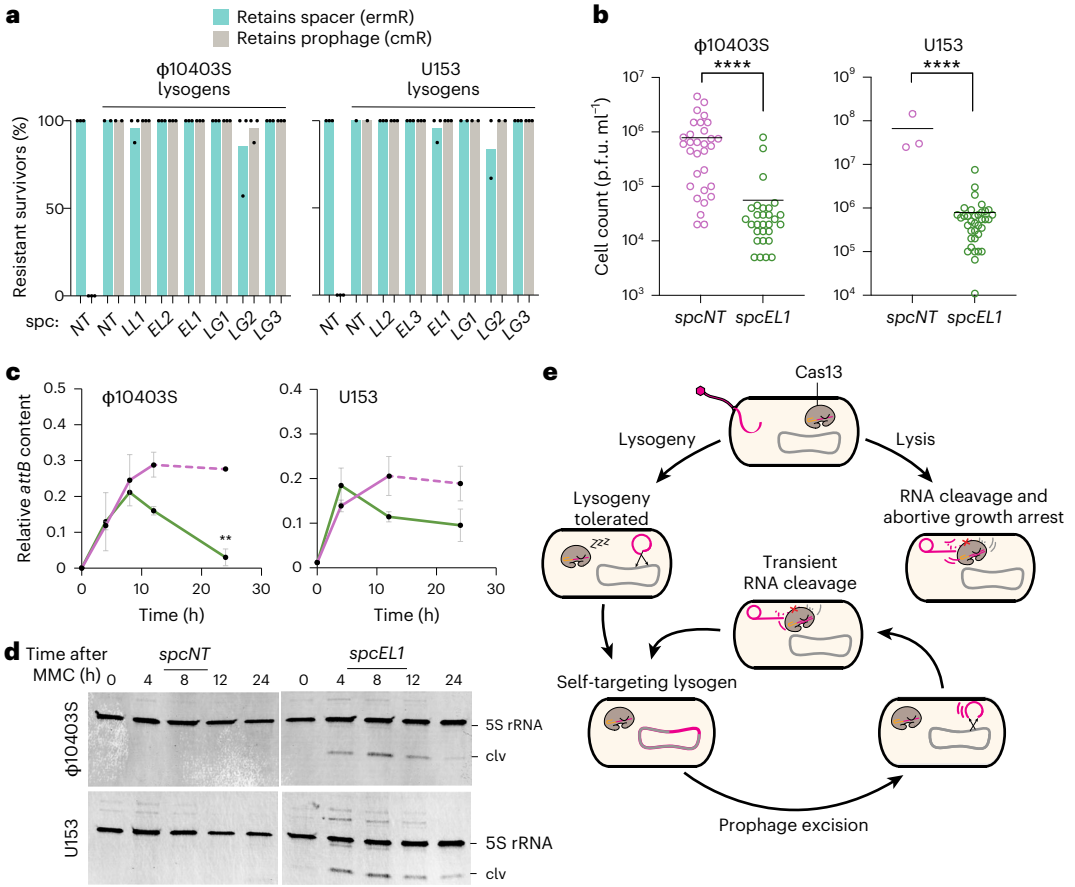

Fig. 4 | Prophage re-integration resolves transient Cas13 activity. **a**,**b**, Surviving colonies from prophage induction were picked and grown in BHI overnight before spotting on BHI with chloramphenicol or erythromycin, or plated for free phage. **a**, The percentage of resistant survivors from three biological replicates are shown along with their means. ermR, erythromycin-resistant; cmR, chloramphenicol-resistant. **b**, Phage titres from overnight cultures of surviving lysogenic colonies (*spcNT*–ϕ10403S, $n = 31$; *spcEL1*–ϕ10403S, $n = 29$; *spcNT*–U153, $n = 3$; *spcEL1*–U153, $n = 36$) from three biological replicate experiments were enumerated. Each circle represents the released p.f.u. of an individual survivor colony. Two-sided Student's *t*-tests were performed to compare the means of the two conditions; $^{****}P < 0.0001$. **c**, Relative *attB* content as measured by qPCR from the indicated cultures following pulsed MMC treatment. Shown are the relative excision values: $2^{-\Delta Cq}$ of the *attB* site calculated by comparing the Cq values from the *attB* site to those from housekeeping gene *ssbA*. The mean and S.E.M of two biological replicates are shown. Student's *t*-tests were performed to compare relative excision values at each point; $^{**}P < 0.01$; no asterisk denotes a non-significant difference. Dashed lines indicate that the culture from which these samples were collected was near complete lysis, due to prophage induction. **d**, Cas13 activity measurement by northern blot for 5S rRNA. RNA was extracted from indicated strains during prophage induction and resolved on a denaturing urea gel before blotting with Cy3-labelled probe for the *L. seeligeri* 5S rRNA (clv denotes a rRNA cleavage product formed following Cas13 activation). Shown is a representative blot of two biological replicates. **e**, Model of the type VI-A CRISPR immune response to various stages of the temperate phage life cycle in *L. seeligeri*. Exact *P* values for **b** are as follows: for the ϕ10403S comparison, $P = 4.22 \times 10^{-5}$; for the U153 comparison, $P = 3.58 \times 10^{-8}$.

While type VI-A CRISPR systems restrict lytic infection via an abortive mechanism, our data show that Cas13 restricts prophage induction in a cell-autonomous manner.

Prophage re-integration resolves the type VI-A CRISPR immune response

We reasoned that, following type VI-A-mediated restriction of prophage induction, the Cas13 immune response could be resolved through loss of the targeted prophage, or through prophage re-integration and silencing of the target RNA. To determine whether survivors of induction retained the targeted prophage and immunity plasmid, we tested individual colonies for chloramphenicol resistance encoded by the phage and erythromycin resistance encoded by the integrated spacer plasmid. We saw that nearly all survivors from targeted prophage induction retained both prophage and plasmid (Fig. 4a). Furthermore, surviving lysogens still produced detectable virions via spontaneous induction, and those with a *spcEL1* spacer produced fewer p.f.u., indicating that both the prophage and Cas13 immunity remain functional following targeted prophage induction (Fig. 4b). Thus, type VI-A immunity limits prophage induction while retaining the prophage and functional immune system. Next, we asked whether Cas13-mediated interference occurs before or after prophage excision from the host chromosome. We performed qPCR at the bacterial attachment locus (*attB*) which is re-formed during prophage excision. We observed a similar degree of *attB* formation in *spcNT* and *spcEL1* strains for both ϕ10403S and U153 prophages. However, at later time points, *attB* site abundance decreases in the *spcEL1* lysogen, suggesting that Cas13 does not impair initial prophage excision but later enforces prophage re-integration and re-occupation of the *attB* site (Fig. 4c). We note that at the latest time point, the *spcNT* cultures showed near-complete lysis, making it difficult to compare *attB* content between *spcNT* and *spcEL1* conditions (Fig. 4c, dashed lines). We also tracked phage genome abundance by performing qPCR at the phage attachment site (*attP*) formed on the phage chromosome after excision and replication. We detected initial *attP* reconstitution and some phage genome replication but Cas13-dependent reduction of *attP* content at later time points, consistent with re-integration and a restriction of phage genome replication (Extended Data Fig. 9). Finally, we directly measured Cas13 activation

https://doi.org/10.1038/s41564-026-02288-5

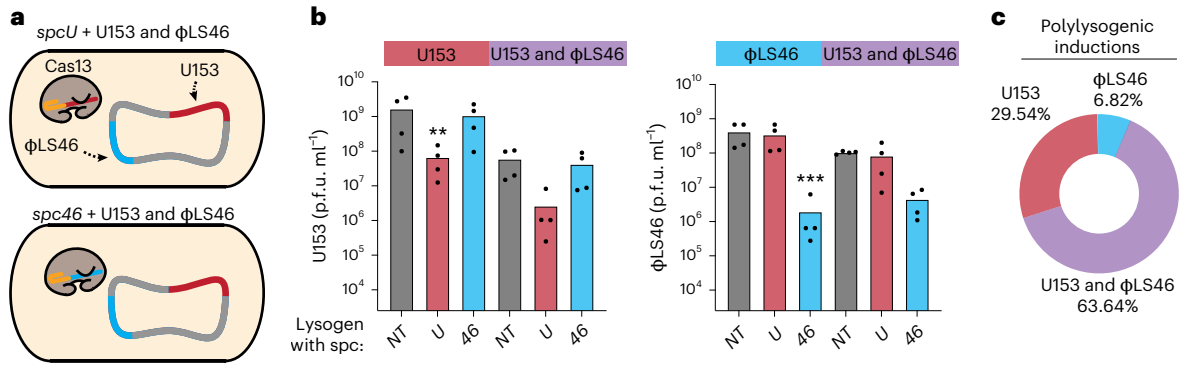

Fig. 5 | Cas13 specifically restricts targeted phages during polylysogenic induction. a, Diagrams of *L. seeligeri* with different polylysogenic backgrounds with either spacer targeting U153 (*spcU*) or spacer targeting ϕLS46 (*spc46*). **b**, The indicated self-targeting lysogens were diluted into BHI + 2 mg ml^{-1} MMC; p.f.u. corresponding to each phage were enumerated at 8 h after treatment on selective lawns harbouring type II-A CRISPR spacers against either U153 or ϕLS46. Four biological replicates and mean are shown. One-way ANOVA analysis with Dunnet's test was performed on each column, comparing the means of either targeting lysogen compared to the corresponding non-targeting lysogen or non-targeting polylysogen. $^{**}P < 0.01$ denotes a significant difference between the indicated column and the *spcNT* control column; $^{***}P < 0.001$; no asterisk represents a non-significant difference. **c**, To determine whether phages are reactivating in the same cell, polylysogens with a non-targeting spacer were treated with MMC, washed of free phage and plated on a susceptible lawn before lysis. Plaques formed on these lawns were then isolated and plated on selective lawns to analyse their composition. Shown are the means of three biological replicates. Exact *P* values for **b** are as follows: for released U153 phage, $P = 0.0023$ for *spcU* in a U153 lysogen; the $P = 0.0002$ for *spc46* in a ϕLS46 lysogen.

during induction of targeted prophages by performing northern blots on 5S ribosomal RNA, a known Cas13 cleavage substrate. We saw transient Cas13-dependent 5S rRNA cleavage during induction of each prophage in the presence of *spcEL1* (Fig. 4d). Together, these data support a model in which targeted prophages activate Cas13 after excision, resulting in transient non-specific RNA cleavage, which is resolved following prophage re-integration and silencing of the stimulatory mRNA (Fig. 4e).

Integration and excision of A118-like *Listeria* prophages, including ϕ10403S, is catalysed by a large serine recombinase (Int) and accompanying recombination directionality factor (RDF)[25]. In isolation, Int catalyses integration, but upon interaction with RDF, Int–RDF catalyses excision. As such, Cas13-mediated depletion of RDF represents one possible mechanism driving prophage re-integration during reactivation of targeted prophages. To investigate this, we monitored *int* and *rdf* transcript levels by RT-qPCR following MMC treatment in self-targeting or non-targeting lysogens. Levels of both transcripts increased during prophage induction, and neither were significantly depleted during Cas13 targeting (Extended Data Fig. 10a). We then generated functionally tagged RDF and Int alleles in ϕ10403S lysogens equipped with the *spcNT* or *spcEL1* construct and monitored protein abundance following MMC treatment. We found that RDF synthesis gradually increases during reactivation, but levels did not differ between the *spcNT* and *spcEL1* background (Extended Data Fig. 10b). Although the tagged Int protein functioned in catalysing excision, we were unable to detect it via immunoblotting. Together, these data argue that Cas13-mediated prophage re-integration does not require specific depletion of RDF.

Cas13 immunity is specific during multiple prophage induction

Many *L. seeligeri* strains are polylysogens, harbouring multiple prophages which can be co-induced by DNA damage[26]. Once activated by target mRNA, Cas13 restricts both targeted and non-targeted phages during lytic infection through non-specific RNA degradation[21]. Hence, we were interested in whether non-targeted phages are similarly restricted during polylysogen induction. To this end, we engineered polylysogens harbouring both U153 and another temperate listeriaphage with a separate integration site, ϕLS46 (Extended Data Fig. 1). We then separately introduced a non-targeting spacer (*spcNT*), a spacer targeting U153 (*spcU*) or a spacer targeting ϕLS46 (*spc46*) into the polylysogen strain (Fig. 5a). We treated these self-targeting polylysogens with MMC and enumerated released U153 or ϕLS46 phage on selective lawns equipped with Cas9 directed against each individual phage. Using this system, we found that polylysogens produce fewer virions of each individual phage than their monolysogenic counterparts, possibly due to competition for resources within the cell (Fig. 5b). Furthermore, we found that Cas13 restricts induction of the targeted prophage but not the untargeted prophage during polylysogen induction (Fig. 5b). One explanation for these observations is that the two prophages never reactivate in the same cell, precluding any opportunity for non-specific restriction. To test this, we isolated *spcNT* polylysogenic cells treated with MMC before lysis, repeatedly washed away free phage and plated on a non-selective lawn. We then isolated resultant plaques and plated them on selective lawns to determine whether individual inducing cells gave rise to either one or both phages. We found that most reactivating polylysogens produced hybrid plaques containing both phages (Fig. 5c), supporting the idea that both prophages are broadly induced in the same cell. Thus, our evidence suggests that Cas13 acts in such a limited or transient fashion in an inducing polylysogen that it is incapable of restricting the induction of a non-targeted prophage.

Discussion

Here we have shown that the type VI-A CRISPR system tolerates lysogeny while restricting lytic infection and prophage induction, through conditional activation of Cas13. We find that the effects of Cas13 vary in each stage of the temperate phage life cycle. During lytic infection, Cas13 elicits a prolonged growth arrest from which cells do not recover. During lysogeny, Cas13 remains inactive as lysogenic target RNAs do not exceed the threshold required to trigger RNA cleavage, and thus, prophage acquisition is tolerated. During prophage induction, we observe transient Cas13 activation after prophage excision, which blocks lysis and is resolved by re-integration of the prophage into the *attB* site. It can be inferred from the data in Fig. 1c that phage restricted during lytic infection cannot enter the lysogenic pathway to resolve the Cas13 response, unlike targeted phages undergoing induction. If this were the case, we would expect an increase in lysogen establishment during Cas13 activation. Instead, we measured similar lysogeny rates under targeting and non-targeting conditions, suggesting that infecting phages cannot switch from lytic to lysogenic replication, in contrast to inducing phages. Finally, while the non-specific nature of Cas13-mediated RNA cleavage neutralizes both targeted and non-targeted phage during lytic co-infection[21], we found

that Cas13 interferes specifically against targeted prophages during polylysogenic induction.

What drives prophage re-integration during the type VI-A immune response following induction? Excision is driven by Int in complex with its RDF co-factor. We observe that excision is unaffected by Cas13 targeting, and thus, both Int and RDF are produced. We found that re-integration during Cas13 targeting is not accompanied by a loss of RDF. We speculate that the replication-arrested prophage is a prime substrate for free Int, which may dissociate from RDF at some constant rate, switching the polarity of the enzyme to favour integration. This ability of the ϕ10403S prophage to excise and reintegrate has been shown to play a role in regulating *Listeria monocytogenes* pathogenesis[5]. In this case, phage replication arrest is caused by inhibition of an activator of late gene expression. For the prophage, re-integration may serve as a mechanism to ensure its maintenance when induction is arrested. During Cas13-induced re-integration, Cas13 activation is evident by 5S rRNA cleavage, but we detected no concomitant growth arrest, suggesting that re-integration occurs rapidly within single cells. Overall, this pathway to resolve the type VI-A immune response allows Cas13-equipped hosts to benefit from potential fitness advantages conferred by prophages while mitigating liabilities associated with autoimmune self-targeting, or phage-induced lysis. We have previously shown that primed acquisition rapidly generates type VI-A spacers targeting an integrated prophage[27]. Thus, self-targeting lysogens can be formed both by integration of a CRISPR-targeted prophage or by spacer acquisition from a resident prophage. How type VI-A self-targeting affects prophage accumulation or the formation of cryptic prophages remain open questions. Broadly, CRISPR systems can present a strong barrier to lysogeny[13,18,28,29]. Some recently described non-CRISPR defences have been shown to tolerate prophages, yet their mechanisms of action remain to be elucidated[30,31]. Further study of novel bacterial immune systems' interactions with temperate phages may lead to the discovery of emergent prophage-tolerant behaviours. Characterization of prophage-tolerant immune systems and their distribution could deepen our understanding of virulence trait acquisition and evolution in bacterial populations.

Methods

Bacterial strains and growth conditions

L. seeligeri strains were derived from American Type Culture Collection strain 35967 (Rocourt and Grimont) and were grown in brain heart infusion (BHI) broth or agar at 30 °C. Where appropriate, BHI was supplemented with the following antibiotics for selection: nalidixic aid (50 μg ml^{-1}), chloramphenicol (10 μg ml^{-1}), erythromycin (1 μg ml^{-1}) or kanamycin (50 μg ml^{-1}). For cloning, plasmid preparation and conjugative plasmid transfer, *E. coli* strains were cultured in lysogeny broth (LB) medium at 37 °C. Where appropriate, LB was supplemented with the following antibiotics: ampicillin (100 μg ml^{-1}), chloramphenicol (25 μg ml^{-1}), or kanamycin (50 μg ml^{-1}). For conjugative transfer of *E. coli–Listeria* shuttle vectors, plasmids were purified from Turbo competent *E. coli* (New England Biolabs) and transformed into the *E. coli* conjugative donor strain S-17 λ*pir*.

Phage propagation

All phage infections were performed in BHI medium supplemented with 5 mM $CaCl_2$. To generate phage stocks, purified plaques and tenfold serial dilutions were combined with 100 μl of a saturated overnight culture of *L. seeligeri ΔRM1 ΔRM2 ΔCRISPR* in 5 ml of BHI soft agar (0.7% agar) with 5 mM $CaCl_2$, overlayed on a BHI plate. Propagated phages were collected from the fully cleared plate made from the lowest dilution of phage by adding 5 ml of BHI media to the plate, rocking for 10 min, and filtering the resulting phage stock through a 0.45 μm pore syringe filter.

Plasmid construction and preparation

All genetic constructs for expression in *L. seeligeri* were cloned into the following three shuttle vectors, each containing an origin of transfer sequence for mobilization by transfer genes of the Inc-type plasmid RP4: (1) pPL2e—single-copy plasmid conferring erythromycin resistance that integrates into the $tRNA^{Arg}$ locus in the *L. seeligeri* chromosome[32]; (2) pAM8—*E. coli–Listeria* shuttle vector conferring chloramphenicol resistance[33]; and (3) pAM326—*E. coli–Listeria* shuttle vector conferring kanamycin resistance[34]. These transfer genes are integrated into the genome of *E. coli* conjugative donor strains S-17 λ*pir*. Spacer constructs were made through ligation of annealed oligos containing the spacer sequence into digested pPL2e derivatives, pAM305 for type VI-A spacers and pAM287 for type II-A. All other plasmids were constructed from shuttle vectors via Gibson assembly of restriction digested or PCR-amplified backbones with PCR-amplified inserts. Details of plasmid construction, along with plasmid information and oligonucleotides used in this study, are also found in Supplementary Table 1.

E. coli–L. seeligeri conjugation

Donor *E. coli* strains S-17 λ*pir* carrying *E. coli–Listeria* shuttle vectors were cultured overnight in LB medium with the appropriate antibiotic: 25 μg ml^{-1} chloramphenicol (for pPL2e-derived plasmids), 50 μg ml^{-1} kanamycin (for pAM326-derived plasmids) or 100 μg ml^{-1} ampicillin (for pAM8-derived plasmids). Recipient *L. seeligeri* strains were grown overnight in BHI medium supplemented with 1 μg ml^{-1} erythromycin (for pPL2e-derived plasmids), 10 μg ml^{-1} chloramphenicol (for marked lysogens or pAM8-derived plasmids) or 50 μg ml^{-1} kanamycin (for pAM326-derived plasmids) at 30 °C. The saturated donor and recipient cultures (100 μl each) were combined in 10 ml of BHI and concentrated onto a 0.45 μm membrane filter disc (Millipore-Sigma) using vacuum filtration. The filter was then placed on BHI agar containing 8 μg ml^{-1} oxacillin (or 128 μg ml^{-1} when conjugating pAM8-derived plasmids), which weakens the cell wall, enhancing conjugation, and incubated at 37 °C for 4 h. After incubation, the cells were resuspended in 2 ml of BHI and plated on selective BHI medium containing 50 μg ml^{-1} nalidixic acid, which kills donor *E. coli* but not recipient *Listeria*, along with the appropriate antibiotic for plasmid selection. Transconjugants were isolated after 2–3 days of incubation at 30 °C.

Phage engineering

Repair plasmids were generated via Gibson assembly with PCR-amplified pAM326, 1 kb homology arms amplified from the respective phage, and cargo gene fragments to be inserted. Repair plasmids were conjugated into *L. seeligeri*, and the resulting transconjugants were infected with either U153 or ϕ10403S to enable recombination between the phage and repair plasmid. The resulting phage lysate was purified, and recombinants were selected by Cas9 counterselection using pAM307-derived plasmids or by infection of fresh cultures of *L. seeligeri* at an MOI of 0.1 for 30 min and selection for chloramphenicol-resistant lysogens on BHI + chloramphenicol in the case where genetic insertions included the *catA* gene. A stock of recombinant phage was then produced by expanding a plaque arising on a counterselection lawn or a plaque derived from the supernatant of an overnight culture grown from a chloramphenicol-resistant lysogen.

Lysogen establishment assays

Overnight cultures of strains to be lysogenized were grown in 5 ml of BHI, incubated at 30 °C overnight. Cultures were grown to an OD_{600} of 0.5–1.0 before being back diluted to an OD_{600} of 0.05 in 500 μl of BHI supplemented with 5 mM $CaCl_2$. Phages engineered with *catA* were then added to a MOI of 0.3 and allowed to incubate at 30 °C for 30 min. Infected cells were then pelleted by centrifugation for 3 min at 6,000 × *g*; the supernatant was decanted, and the cell pellet was resuspended in 500 μl of BHI supplemented with 100 mM sodium citrate. Tenfold serial dilutions of infected cells were made in BHI + sodium citrate, and 100 μl of diluted and undiluted samples were spread on BHI supplemented with chloramphenicol and sodium citrate. Lysogenic colonies appeared after 2–3 days of incubation at 30 °C.

Cas13 induction experiments

Overnight cultures of LS1 94˚::P_{tet}-*pspc4* were grown in 5 ml of BHI and incubated at 30 °C overnight. Overnight cultures were diluted to an OD_{600} of 0.05 in 5 ml of BHI and treated with 100 ng ml^{-1} aTc for 30 min where appropriate to induce targeted protospacer transcription. Induced or uninduced cultures were then infected with U153 or ϕ10403S at an MOI of 0.1 for 6 h; resulting lysogenic cells or p.f.u. were then enumerated on BHI supplemented with chloramphenicol and sodium citrate, or a lawn of *L. seeligeri ΔRM1 ΔRM2 ΔCRISPR*, respectively.

Prophage induction experiments

Overnight cultures of strains to be treated with MMC were grown in 5 ml of BHI and incubated at 30 °C overnight. Cultures were grown to an OD_{600} of 0.5–1.0 before being diluted to an OD_{600} of 0.1 in BHI containing MMC. For Figs. 3b,c and 5, cultures were diluted into BHI supplemented with 2 μg ml^{-1} MMC sodium salt (Sigma Aldrich); p.f.u. were measured after 8 h by plating 2 μl dilution spots on lawns of *L. seeligeri ΔRM1 ΔRM2 ΔCRISPR*, and viable c.f.u. were measured where applicable after 24 h by plating 5 μl dilution spots onto BHI supplemented with sodium citrate. For Figs. 3d and 4, cultures were diluted into BHI supplemented with 1 μg ml^{-1} MMC in DMSO (Sigma Aldrich) for 30 min before being pelleted by centrifugation and washed twice with fresh BHI. Released p.f.u. and surviving cells were measured as described above, and cell pellets were collected at 0, 4, 8, 12 and 24 h.

qPCR

DNA was isolated from 1 ml of the indicated *L. seeligeri* cultures during MMC treatment by lysozyme treatment and phenol-chloroform extraction. qPCR was performed with 100 ng template DNA using iTaq Universal SYBR Green Supermix (Bio-Rad), the appropriate primer pair amplifying *attB*, *attP* or housekeeping *ssbA* DNA loci, and a Bio-Rad CFX384 Touch Real-Time PCR Detection System. Relative abundance of either *attB* or *attP* sites were calculated by subtracting the Cq value of the *ssbA* locus at the matched time point (ΔCq). Relative abundance values in each time course were normalized to the starting *attB* or *attP* content, which was set to 0.

Northern blot

RNA was isolated from 1 ml of the indicated *L. seeligeri* cultures during MMC treatment using the Direct-zol RNA Miniprep kit (Zymo Research). RNA was mixed with an equal volume of 2× RNA loading dye (95% formamide, 18.8 mM EDTA and 0.02% bromophenol blue), heated to 95 °C for 3 min and then cooled on ice for 1 min. Then, 1 μg total RNA from each sample was resolved by denaturing 15% TBE-urea PAGE and was transferred overnight to BrightStar nylon membranes (Invitrogen). Membranes were UV-crosslinked, then pre-hybridized in 2× SSC + 1% SDS in hybridization oven at 42 °C for 30 min, followed by the addition of 250 pmol Cy3-labelled single-stranded DNA probe and overnight incubation at 42 °C. Hybridized membranes were washed twice with 2× SSC + 0.1% SDS for 5 min then once with 1× SSC + 0.1% SDS for 20 min in hybridization oven at 42 °C and then scanned on an Azure Sapphire imager.

Microscopy

Phage infections were performed with mid-exponential-phase cells infected at an OD_{600} of 0.05 and MOI 50 in 500 μl of BHI supplemented with 5 mM $CaCl_2$. Infected cells were incubated at 30 °C for 30 min before being pelleted by centrifugation and washed in 500 μl of BHI. Infected cells were then loaded into microfluidic chambers using the CellASIC ONIX2 microfluidic system (Millipore Sigma). After cells became trapped in the chamber, BHI media was supplied under a constant flow rate of 5 μl h^{-1}. Phase contrast images were captured at ×1,000 magnification every 30 min for 12 h after infection, using a Nikon Ti2e inverted microscope equipped with a Hamamatsu Orca-Fusion SCMOS camera and temperature-controlled enclosure set to 30 °C. mStayGold expression was visualized using a GFP filter set and Excelitas Xylis LED Illuminator set to 10% power with an exposure time of 250 ms. Time lapse images were aligned and processed using NIS Elements software v5.3. Quantitative analysis of cell fates were performed in Fiji v2.3.0 (ref. 35). To quantify the fates of infected cells under the microscope, we manually tracked and counted cells that underwent lysis, lysogeny, outgrowth or Cas13-induced growth arrest. Cells that ruptured during imaging were assigned as lytic events; those that expressed phage-encoded mStayGold but continued actively dividing without lysis were assigned as lysogenic events. Cells that continued growing without fluorescence were labelled as outgrowth. Cells that did not divide for the course of imaging were labelled as arrested cells.

RNA-seq and analysis

LS1 was grown in 5 ml of BHI overnight at 30 °C. Mid-exponential-phase cultures were then diluted to an OD_{600} of 0.1 and infected at an MOI of 2 in 10 ml of BHI supplemented with 5 mM $CaCl_2$. At 0, 30 and 120 min after infection, 2 ml of the culture was collected, and total RNA was extracted using the Direct-zol RNA Miniprep kit (Zymo Research). Ribosomal RNA depletion, Illumina library preparation and 2 × 150 paired-end Illumina RNA-seq was performed by SeqCenter. Reads were then mapped to the corresponding genome using bowtie2 using default settings.

Reporting summary

Further information on research design is available in the Nature Portfolio Reporting Summary linked to this article.

Data availability

All RNA-sequencing data reported here have been uploaded to NCBI under BioProject accession number PRJNA1414806. Lists of strains, plasmids and oligonucleotides used in this study are available in Supplementary Table 1. Further information and requests for resources and reagents should be directed to and will be fulfilled by the corresponding author. Source data are provided with this paper.

References

1. Bernheim, A. & Sorek, R. The pan-immune system of bacteria: antiviral defence as a community resource. *Nat. Rev. Microbiol.* **18**, 113–119 (2020).
2. López-Leal, G. et al. Mining of thousands of prokaryotic genomes reveals high abundance of prophages with a strictly narrow host range. *mSystems* **7**, e00326-22 (2022).
3. Calendar, R. & Abedon ST. *The Bacteriophages* (Oxford Univ. Press, 2005).
4. Oppenheim, A. B., Kobiler, O., Stavans, J., Court, D. L. & Adhya, S. Switches in bacteriophage lambda development. *Annu. Rev. Genet.* **39**, 409–429 (2005).
5. Pasechnek, A. et al. Active lysogeny in *Listeria monocytogenes* is a bacteria-phage adaptive response in the mammalian environment. *Cell Rep.* **32**, 107956 (2020).
6. Brown, E. M. et al. Gut microbiome ADP-ribosyltransferases are widespread phage-encoded fitness factors. *Cell Host Microbe* **29**, 1351–1365.e11 (2021).
7. Gummalla, V. S., Zhang, Y., Liao, Y.-T. & Wu, V. C. H. The role of temperate phages in bacterial pathogenicity. *Microorganisms* **11**, 541 (2023).
8. Barrangou, R. et al. CRISPR provides acquired resistance against viruses in prokaryotes. *Science* **315**, 1709–1712 (2007).
9. Garneau, J. E. et al. The CRISPR/Cas bacterial immune system cleaves bacteriophage and plasmid DNA. *Nature* **468**, 67–71 (2010).
10. Makarova, K. S. et al. Evolutionary classification of CRISPR–Cas systems: a burst of class 2 and derived variants. *Nat. Rev. Microbiol.* **18**, 67–83 (2020).

11. Edgar, R. & Qimron, U. The *Escherichia coli* CRISPR system protects from λ lysogenization, lysogens, and prophage induction. *J. Bacteriol.* **192**, 6291–6294 (2010).
12. Nozawa, T. et al. CRISPR inhibition of prophage acquisition in *Streptococcus pyogenes*. *PLoS ONE* **6**, e19543 (2011).
13. Rollie, C. et al. Targeting of temperate phages drives loss of type I CRISPR–Cas systems. *Nature* **578**, 149–153 (2020).
14. Goldberg, G. W., Jiang, W., Bikard, D. & Marraffini, L. A. Conditional tolerance of temperate phages via transcription-dependent CRISPR-Cas targeting. *Nature* **514**, 633–637 (2014).
15. Samai, P. et al. Co-transcriptional DNA and RNA cleavage during type III CRISPR-Cas immunity. *Cell* **161**, 1164–1174 (2015).
16. Kazlauskiene, M., Tamulaitis, G., Kostiuk, G., Venclovas, Č & Siksnys, V. Spatiotemporal control of type III-A CRISPR-Cas immunity: coupling DNA degradation with the target RNA recognition. *Mol. Cell* **62**, 295–306 (2016).
17. Elmore, J. R. et al. Bipartite recognition of target RNAs activates DNA cleavage by the type III-B CRISPR-Cas system. *Genes Dev.* **30**, 447–459 (2016).
18. Goldberg, G. W. et al. Incomplete prophage tolerance by type III-A CRISPR-Cas systems reduces the fitness of lysogenic hosts. *Nat. Commun.* **9**, 61 (2018).
19. Abudayyeh, O. O. et al. C2c2 is a single-component programmable RNA-guided RNA-targeting CRISPR effector. *Science* **353**, aaf5573 (2016).
20. Makarova, K. S. et al. An updated evolutionary classification of CRISPR–Cas systems. *Nat. Rev. Microbiol.* **13**, 722–736 (2015).
21. Meeske, A. J., Nakandakari-Higa, S. & Marraffini, L. A. Cas13-induced cellular dormancy prevents the rise of CRISPR-resistant bacteriophage. *Nature* **570**, 241–245 (2019).
22. Williams, M. C. et al. Restriction endonuclease cleavage of phage DNA enables resuscitation from Cas13-induced bacterial dormancy. *Nat. Microbiol.* **8**, 400–409 (2023).
23. Loessner, M. J., Inman, R. B., Lauer, P. & Calendar, R. Complete nucleotide sequence, molecular analysis and genome structure of bacteriophage A118 of *Listeria monocytogenes*: implications for phage evolution. *Mol. Microbiol.* **35**, 324–340 (2000).
24. Vialetto, E. et al. A target expression threshold dictates invader defense and prevents autoimmunity by CRISPR-Cas13. *Cell Host Microbe* https://doi.org/10.1016/j.chom.2022.05.013 (2022).
25. Mandali, S., Gupta, K., Dawson, A. R., Van Duyne, G. D. & Johnson, R. C. Control of recombination directionality by the *Listeria* phage A118 protein Gp44 and the coiled-coil motif of its serine integrase. *J. Bacteriol.* **199**, https://doi.org/10.1128/jb.00019-17 (2017).
26. Silpe, J. E. et al. Small protein modules dictate prophage fates during polylysogeny. *Nature* **620**, 625–633 (2023).
27. Margolis, S. R. & Meeske, A. J. Crosstalk between three CRISPR-Cas types enables primed type VI-A adaptation in *Listeria seeligeri*. *Cell Host Microbe* **33**, 1550–1560 (2025).
28. Nobrega, F. L., Walinga, H., Dutilh, B. E. & Brouns, S. J. J. Prophages are associated with extensive CRISPR–Cas auto-immunity. *Nucleic Acids Res.* **48**, 12074–12084 (2020).
29. Pleška, M., Lang, M., Refardt, D., Levin, B. R. & Guet, C. C. Phage–host population dynamics promotes prophage acquisition in bacteria with innate immunity. *Nat. Ecol. Evol.* **2**, 359–366 (2018).
30. Owen, S. V. et al. Prophages encode phage-defense systems with cognate self-immunity. *Cell Host Microbe* **29**, 1620–1633.e8 (2021).
31. Johnson, C. M., Harden, M. M. & Grossman, A. D. Interactions between mobile genetic elements: an anti-phage gene in an integrative and conjugative element protects host cells from predation by a temperate bacteriophage. *PLoS Genet.* **18**, e1010065 (2022).
32. Lauer, P., Chow, M. Y. N., Loessner, M. J., Portnoy, D. A. & Calendar, R. Construction, characterization, and use of two *Listeria monocytogenes* site-specific phage integration vectors. *J. Bacteriol.* **184**, 4177–4186 (2002).
33. Meeske, A. J. & Marraffini, L. A. RNA guide complementarity prevents self-targeting in type VI CRISPR systems. *Mol. Cell* **71**, 791–801.e3 (2018).
34. Meeske, A. J. et al. A phage-encoded anti-CRISPR enables complete evasion of type VI-A CRISPR-Cas immunity. *Science* **369**, 54–59 (2020).
35. Schindelin, J. et al. Fiji: an open-source platform for biological-image analysis. *Nat. Methods* **9**, 676–682 (2012).

Acknowledgements

We are grateful to all members of the Meeske lab for advice and encouragement, especially S. Margolis, as well as members of the Guo, Mitchell and Jordan labs for helpful discussions. Work in the Meeske Lab is supported by National Institute of General Medical Sciences (R35GM142460), National Science Foundation (FAIN2235762) and the University of Washington Royalty Research Fund. A.J.M. is a Rita Allen Foundation Scholar, and M.G. is supported by the National Institutes of Health Training Grant T32AI083203.

Author contributions

This study was conceived by M.G. and A.J.M. M.G. performed all experiments described in the paper. N.W. assisted in cloning and experimentation. M.G. and A.J.M. wrote and edited the paper.

Competing interests

A.J.M. is a co-founder and advisor of Profluent Bio. The other authors declare no competing interests.

Additional information

Extended data is available for this paper at https://doi.org/10.1038/s41564-026-02288-5.

Supplementary information The online version contains supplementary material available at https://doi.org/10.1038/s41564-026-02288-5.

Correspondence and requests for materials should be addressed to Alexander J. Meeske.

Peer review information *Nature Microbiology* thanks Stineke van Houte and the other, anonymous, reviewer(s) for their contribution to the peer review of this work.

https://doi.org/10.1038/s41564-026-02288-5

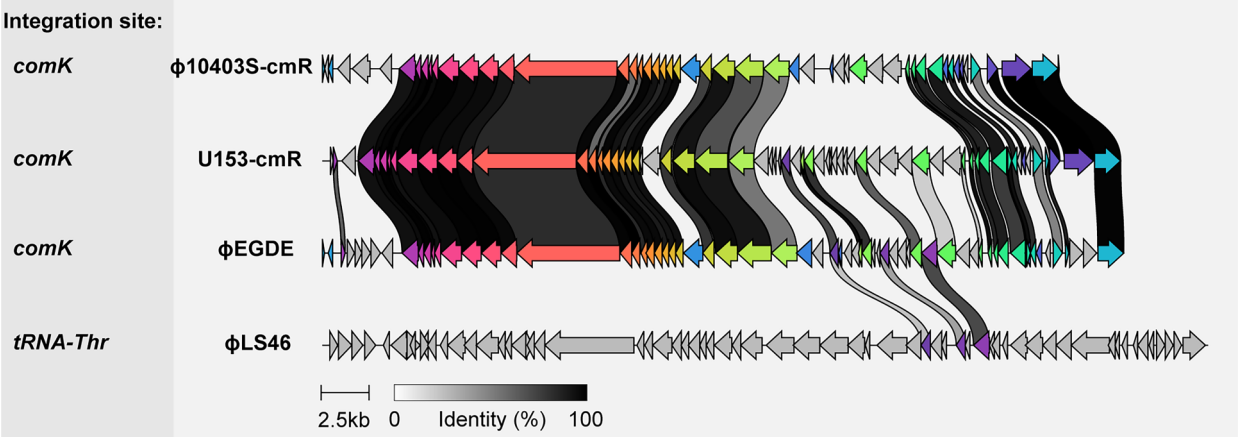

Extended Data Fig. 1 | Relatedness and integration sites of phages used in this study. Genome diagrams of the phages used in this study are aligned with the % nucleotide identity of related genes represented by their shaded connection. Listed in the left column are the *attB* integration sites in the bacterial genome of each phage. Figure was made using clinker & clustermap.

https://doi.org/10.1038/s41564-026-02288-5

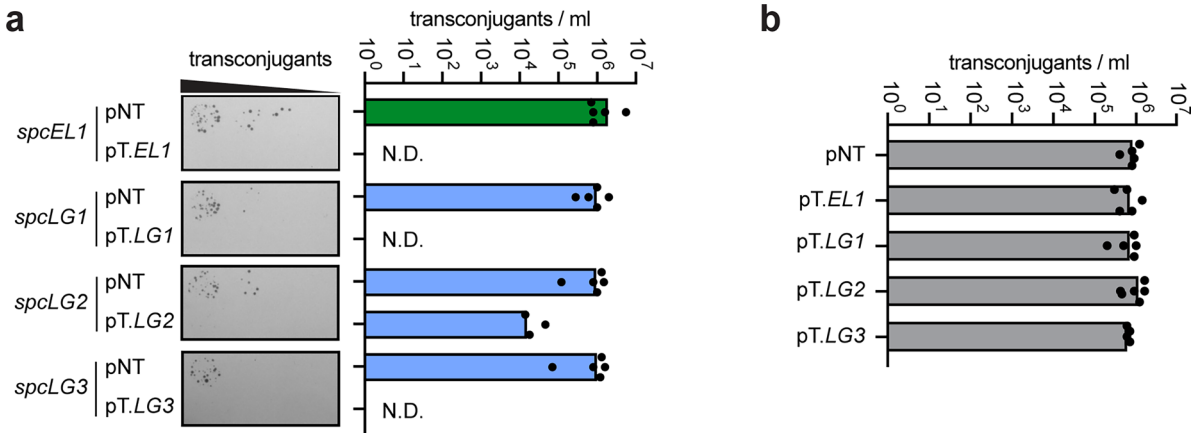

Extended Data Fig. 2 | Spacers sensing lysogenic transcripts are functional in plasmid interference. (**a**) Conjugation assays of either targeted (pT) or non-targeted (pNT) plasmids into *L. seeligeri* with the indicated cognate targeting spacer. Images shown are representative of the five biological replicates quantified. (**b**) Conjugation of target plasmids into a *spcNT* background.

https://doi.org/10.1038/s41564-026-02288-5

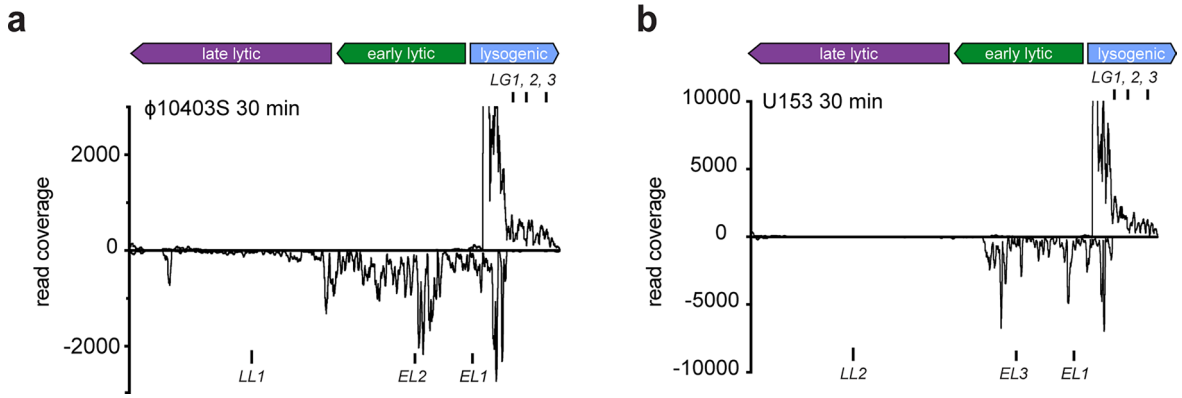

Extended Data Fig. 3 | Lysogenic transcripts targeted by Cas13 are transcribed during bulk infection. RNA-seq was performed on *L. seeligeri* cells 30 min post-infection with U153 or ϕ10403S at an MOI of 2. Reads per nucleotide across the phage genome with the nucleotides corresponding to targeted transcripts highlighted.

https://doi.org/10.1038/s41564-026-02288-5

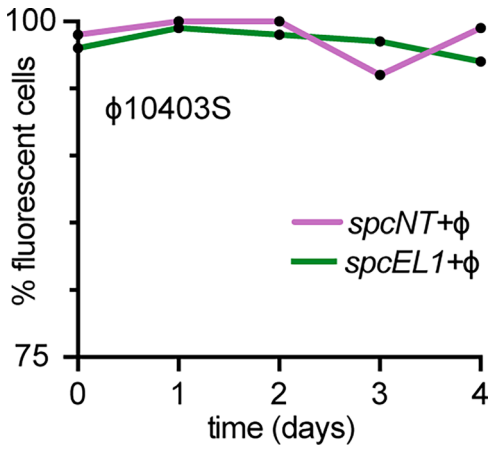

Extended Data Fig. 4 | Self-targeting does not result in prophage loss during passaging of lysogens. Lysogens harboring ϕ10403S- mStayGold in a *spcNT* or *spcEL1* background were passaged daily 100 cells were counted each passage for two replicate cultures in both conditions. Mean of two biological replicates are shown.

https://doi.org/10.1038/s41564-026-02288-5

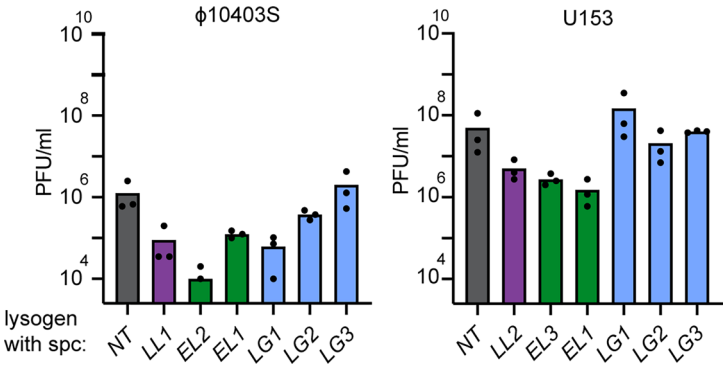

Extended Data Fig. 5 | Cas13 self-targeting reduces spontaneously induced phage in culture. Overnight cultures of the indicated self-targeting or non-targeting lysogens were back diluted in BHI and released PFU were enumerated at 8 h. Three biological replicates are shown.

https://doi.org/10.1038/s41564-026-02288-5

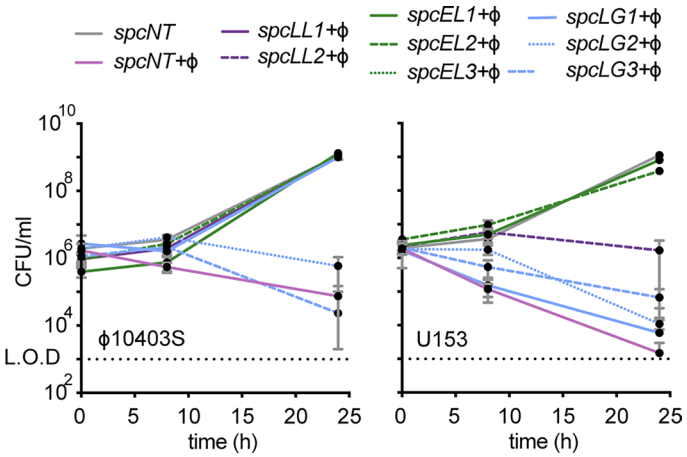

Extended Data Fig. 6 | Select Cas13 spacers block reactivation mediated killing. Time course of viable CFU count after MMC treatment of the indicated strains. Cultures were treated with 2 mg/ml MMC for 60 min before washing and re-suspending in fresh BHI and measuring CFU/ml at the indicated time points. Mean and S.E.M of four biological replicates are shown.

https://doi.org/10.1038/s41564-026-02288-5

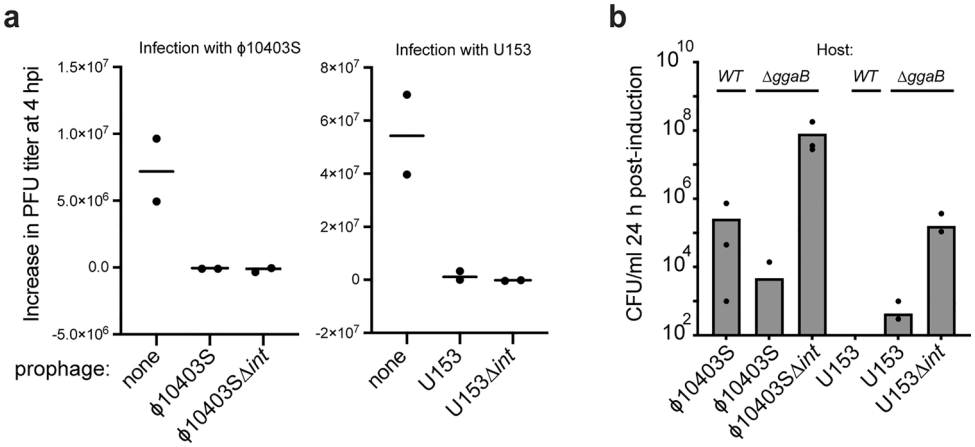

Extended Data Fig. 7 | Lysogen death is due to prophage induction, not super-infection. (**a**) ϕ10403S or U153 lysogens are immune to super-infection. Non-lysogenic *L. seeligeri* or *L. seeligeri* colonized with an active or inactive (Δint) prophage were infected with their cognate phage to determine whether ϕ10403S or U153 provide super-infection exclusion. Cells were infected at an MOI of 0.01 and PFU/ml was measured at 4 h post-infection. Values shown are PFU produced at 4 h subtracted by the input PFU. Mean of two biological replicates is shown. (**b**) Lysogen death after mitomycin C treatment requires prophage excision and is not affected by a phage receptor mutation (Δ*ggaB*). The indicated lysogenic strains were induced with mitomycin C, and viable CFU were enumerated after 24 h. Three biological replicates and their mean are shown.

https://doi.org/10.1038/s41564-026-02288-5

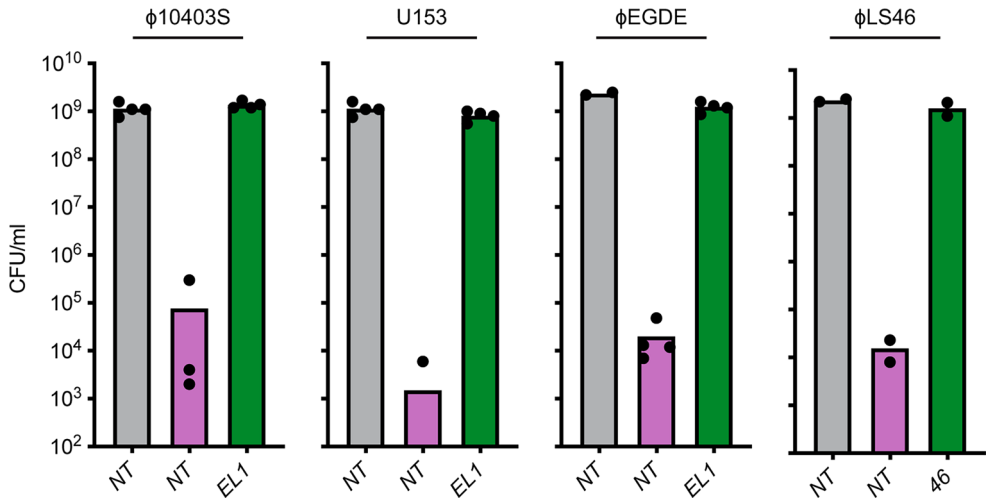

Extended Data Fig. 8 | Cas13 self-targeting promotes survival of diverse lysogens. Surviving CFU were enumerated 24 h after pulsed treatment with mitomycin-C. biological replicates are shown with their means. Columns indicating lysogenic strains are covered by the respective phage they are lysogenized with.

https://doi.org/10.1038/s41564-026-02288-5

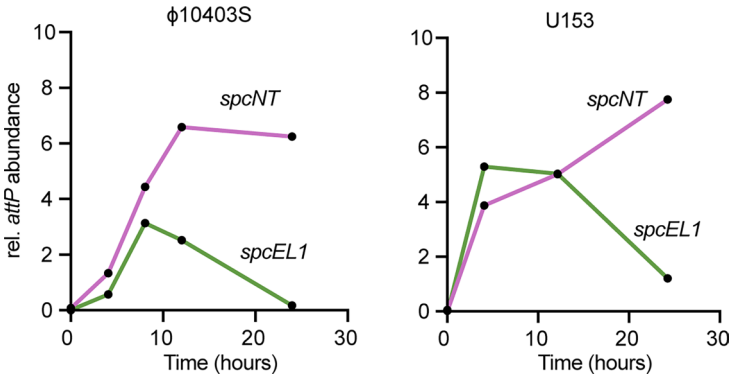

Extended Data Fig. 9 | Prophage genome replication is restricted by Cas13. DNA samples were taken following pulsed MMC treatment and subject to qPCR with primers annealing to the phage attachment (*attP*) site formed during excision and genome replication. Shown are the attP ΔCq values (normalized to the host *ssbA* DNA locus) transformed as such: (2^-ΔCq). The mean of two biological replicates are shown.

https://doi.org/10.1038/s41564-026-02288-5

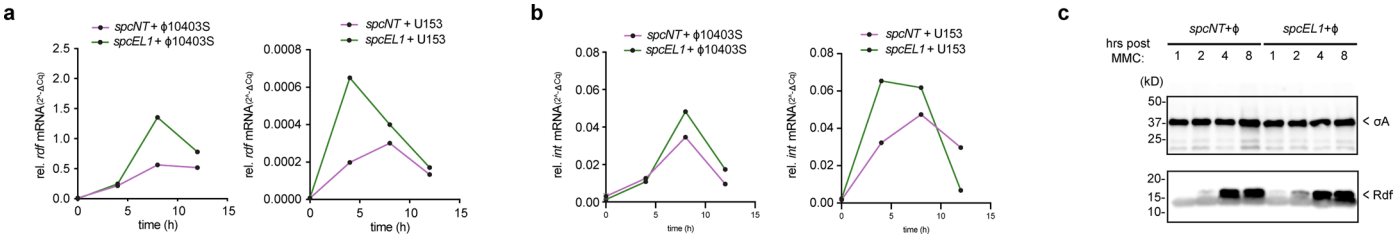

Extended Data Fig. 10 | mRNA and protein levels of relevant integration & excision complex members do not explain prophage re-integration. (**a**), (**b**) RT-qPCRs were performed on RNA extracted from reactivating lysogens with the *NT* or *EL1* spacer, amplifying either recombinase-directionality factor *rdf* locus (a) or integrase (*int*) locus (**b**). Data shown are the mean of two biological replicates. (**c**) Western blots were performed on protein extracted from whole-cell lysates of reactivating lysogens with the *NT* or *EL1* spacer, 3xFLAG tagged Rdf is visualized alongside a σA loading control. Data shown is representative of the two biological replicates analyzed.

nature portfolio

Corresponding author(s): Alex J Meeske

Last updated by author(s): Jan 30, 2026

Reporting Summary

Nature Portfolio wishes to improve the reproducibility of the work that we publish. This form provides structure for consistency and transparency in reporting. For further information on Nature Portfolio policies, see our Editorial Policies and the Editorial Policy Checklist.

Statistics

For all statistical analyses, confirm that the following items are present in the figure legend, table legend, main text, or Methods section.

n/a	Confirmed	
☐	☒	The exact sample size (*n*) for each experimental group/condition, given as a discrete number and unit of measurement
☐	☒	A statement on whether measurements were taken from distinct samples or whether the same sample was measured repeatedly
☐	☒	The statistical test(s) used AND whether they are one- or two-sided *Only common tests should be described solely by name; describe more complex techniques in the Methods section.*
☒	☐	A description of all covariates tested
☒	☐	A description of any assumptions or corrections, such as tests of normality and adjustment for multiple comparisons
☐	☒	A full description of the statistical parameters including central tendency (e.g. means) or other basic estimates (e.g. regression coefficient) AND variation (e.g. standard deviation) or associated estimates of uncertainty (e.g. confidence intervals)
☐	☒	For null hypothesis testing, the test statistic (e.g. *F*, *t*, *r*) with confidence intervals, effect sizes, degrees of freedom and *P* value noted *Give P values as exact values whenever suitable.*
☒	☐	For Bayesian analysis, information on the choice of priors and Markov chain Monte Carlo settings
☒	☐	For hierarchical and complex designs, identification of the appropriate level for tests and full reporting of outcomes
☒	☐	Estimates of effect sizes (e.g. Cohen's *d*, Pearson's *r*), indicating how they were calculated

Our web collection on statistics for biologists contains articles on many of the points above.

Software and code

Policy information about availability of computer code

Data collection	Microscopy data was collected using NIS Elements software (v5.3). Northern blot images were acquired using Azure Biosystems Sapphire control software (v1.0).
Data analysis	Microscopy data was processed using NIS Elements software (v5.3), then analyzed using Fiji (v2.3.0). Contrast of northern blot images was adjusted in Fiji (v2.3.0). Growth curves, CFU and PFU measurements, and bioinformatic data were analyzed in GraphPad Prism 9.bowtie2 was used for read mapping during RNA-sequencing analysis.

For manuscripts utilizing custom algorithms or software that are central to the research but not yet described in published literature, software must be made available to editors and reviewers. We strongly encourage code deposition in a community repository (e.g. GitHub). See the Nature Portfolio guidelines for submitting code & software for further information.

Data

Policy information about availability of data

All manuscripts must include a data availability statement. This statement should provide the following information, where applicable:

- Accession codes, unique identifiers, or web links for publicly available datasets
- A description of any restrictions on data availability
- For clinical datasets or third party data, please ensure that the statement adheres to our policy

Lists of strains, plasmids, and oligonucleotides used in this study are available in Supplementary

Table 2. Further information and requests for resources and reagents should be directed to and will be fulfilled by the corresponding author, Alexander Meeske (meeske@uw.edu).

Research involving human participants, their data, or biological material

Policy information about studies with human participants or human data. See also policy information about sex, gender (identity/presentation), and sexual orientation and race, ethnicity and racism.

Reporting on sex and gender	NA
Reporting on race, ethnicity, or other socially relevant groupings	NA
Population characteristics	NA
Recruitment	NA
Ethics oversight	NA

Note that full information on the approval of the study protocol must also be provided in the manuscript.

Field-specific reporting

Please select the one below that is the best fit for your research. If you are not sure, read the appropriate sections before making your selection.

☒ Life sciences ☐ Behavioural & social sciences ☐ Ecological, evolutionary & environmental sciences

For a reference copy of the document with all sections, see nature.com/documents/nr-reporting-summary-flat.pdf

Life sciences study design

All studies must disclose on these points even when the disclosure is negative.

Sample size	Sample sizes were not statistically predetermined. All experiments were performed with sample sizes based on standard protocols in the field.
Data exclusions	No data were excluded from the analysis.
Replication	All experiments were performed with three biological replicates unless stated otherwise. All attempts at replication were successful. Performed twice - Fig, 4c, 4d, Extended Data Fig 4, 7, 8, 10C Performed once - Extended Data Fig. 2
Randomization	Not relevant to this study.
Blinding	Not relevant to this study.

Reporting for specific materials, systems and methods

We require information from authors about some types of materials, experimental systems and methods used in many studies. Here, indicate whether each material, system or method listed is relevant to your study. If you are not sure if a list item applies to your research, read the appropriate section before selecting a response.

Materials & experimental systems

n/a	Involved in the study
☒	☐ Antibodies
☒	☐ Eukaryotic cell lines
☒	☐ Palaeontology and archaeology
☒	☐ Animals and other organisms
☒	☐ Clinical data
☒	☐ Dual use research of concern
☒	☐ Plants

Methods

n/a	Involved in the study
☒	☐ ChIP-seq
☒	☐ Flow cytometry
☒	☐ MRI-based neuroimaging

Plants

Seed stocks

Report on the source of all seed stocks or other plant material used. If applicable, state the seed stock centre and catalogue number. If plant specimens were collected from the field, describe the collection location, date and sampling procedures.

Novel plant genotypes

Describe the methods by which all novel plant genotypes were produced. This includes those generated by transgenic approaches, gene editing, chemical/radiation-based mutagenesis and hybridization. For transgenic lines, describe the transformation method, the number of independent lines analyzed and the generation upon which experiments were performed. For gene-edited lines, describe the editor used, the endogenous sequence targeted for editing, the targeting guide RNA sequence (if applicable) and how the editor was applied.

Authentication

Describe any authentication procedures for each seed stock used or novel genotype generated. Describe any experiments used to assess the effect of a mutation and, where applicable, how potential secondary effects (e.g. second site T-DNA insertions, mosiacism, off-target gene editing) were examined.